Supplementary Information

In Situ Self-Assembly of Silver Nanoparticles

Boris B. Bokhonov[1], Marat R. Sharafutdinov[1], David R. Whitcomb[2], and Lilia P. Burleva[2]*

[1]Institute of Solid State Chemistry, Siberian Branch, Russian Academy Sciences, Kutateladze 18, 630128 Novosibirsk, Russia

[2]Carestream Health, Inc., 1 Imation Way, Oakdale, MN 55128, USA

* Address correspondence to: bokhonov@solid.nsc.ru

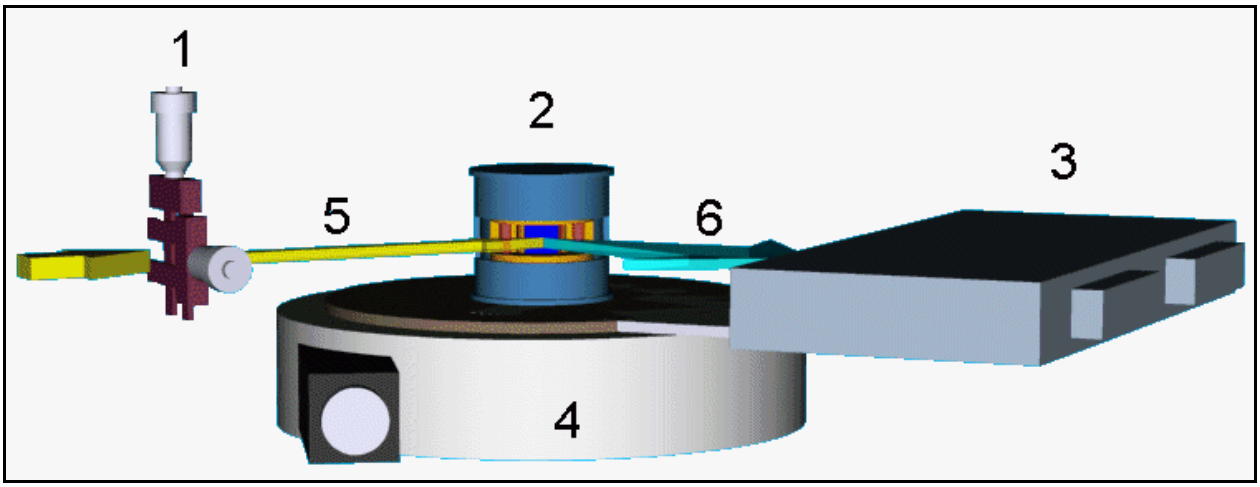

Figure S1. Schematic of the set-up at the synchrotron radiation diffraction station. 1 – system of slits, 2 – furnace with the sample, 3 – detector OD-3, 4 - goniometer, 5 – incident beam, 6 – diffracted beam.

In situ **time-resolved x-ray diffraction during thermal decomposition of C14, C16 and C22 silver carboxylates**

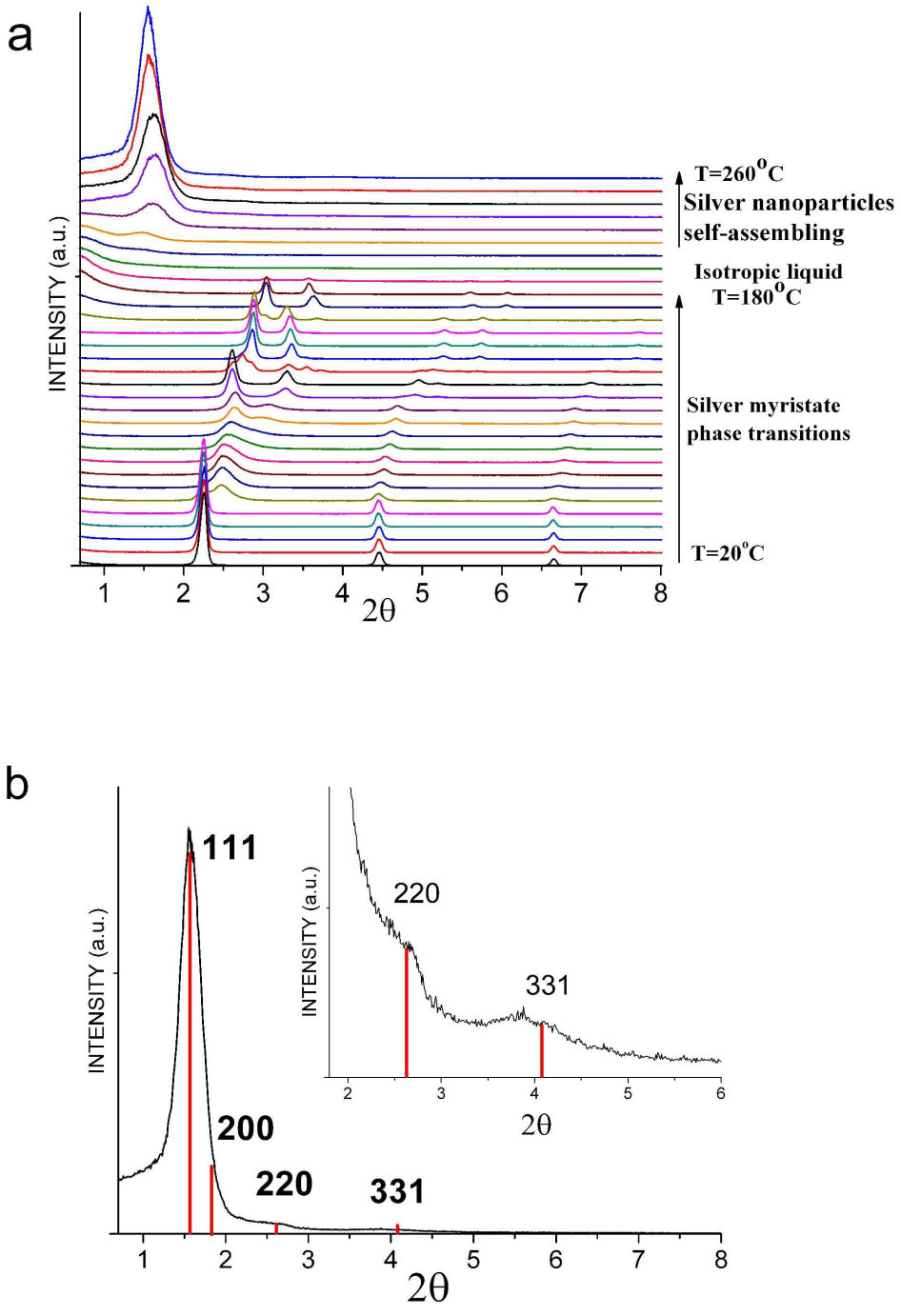

Figure S2.

a. *In situ* time-resolved X-ray diffraction during thermal decomposition of silver myristate (C14). The change in diffraction patterns during heating from 20 °C to 180 °C are caused by multiple phase transitions of silver carboxylates into various liquid-crystalline states. The transition at ~180 °C is the conversion into an isotopic liquid, which is accompanied by the complete disappearance of Bragg reflections. The change of diffraction patterns during heating higher than 200°C corresponds to the formation of ordered silver nanoparticles in an FCC nanostructure.

b. Small-angle X-ray diffraction pattern of self-assembled structures of silver nanoparticles forming during thermal decomposition of silver myristate (C14) at 250°C are indexed as an FCC structure. Magnified portions of the diffraction patterns are shown in the inserts. Calculated unit cell parameter: a = 9.55 nm.

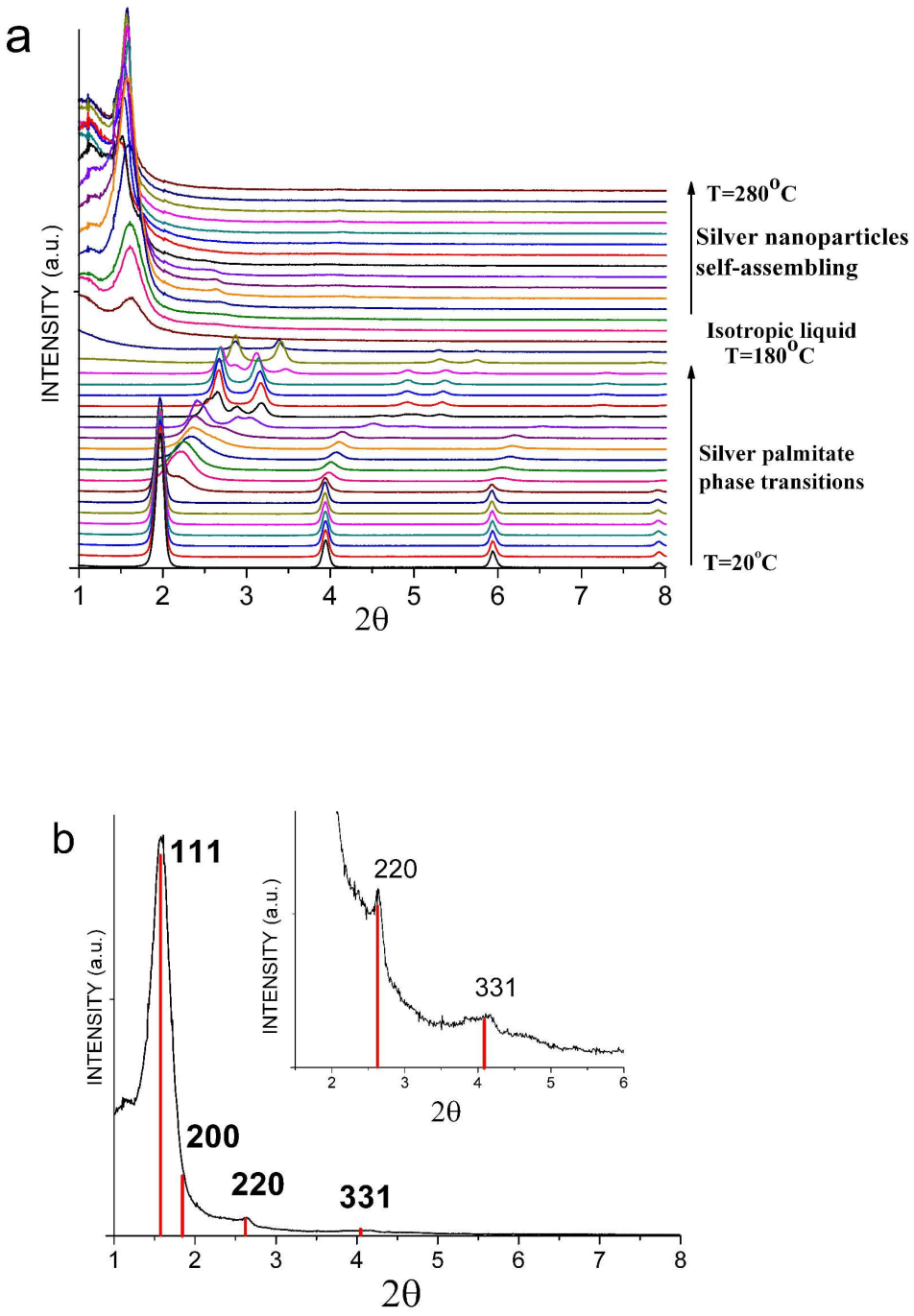

Figure S3.

a. *In situ* time-resolved X-ray diffraction patterns during thermal decomposition of silver palmitate (C16). The changes in the diffraction patterns during heating from 20°C to 180°C are

caused by multiple phase transitions of silver carboxylates into various liquid-crystalline states. The transition at ~180°C is the conversion into an isotopic liquid, which is accompanied by the complete disappearance of Bragg reflections. The change of diffraction patterns during heating higher than 200°C corresponds to the formation of ordered silver nanoparticles in an FCC nanostructure.

b. Small-angle X-ray diffraction pattern of self-assembled structures of silver nanoparticles forming during thermal decomposition of silver palmitate (C16) at 250°C are indexed as an FCC structure. Magnified portions of the diffraction patterns are shown in the inserts. Calculated unit cell parameter: a = 9. 8 nm.

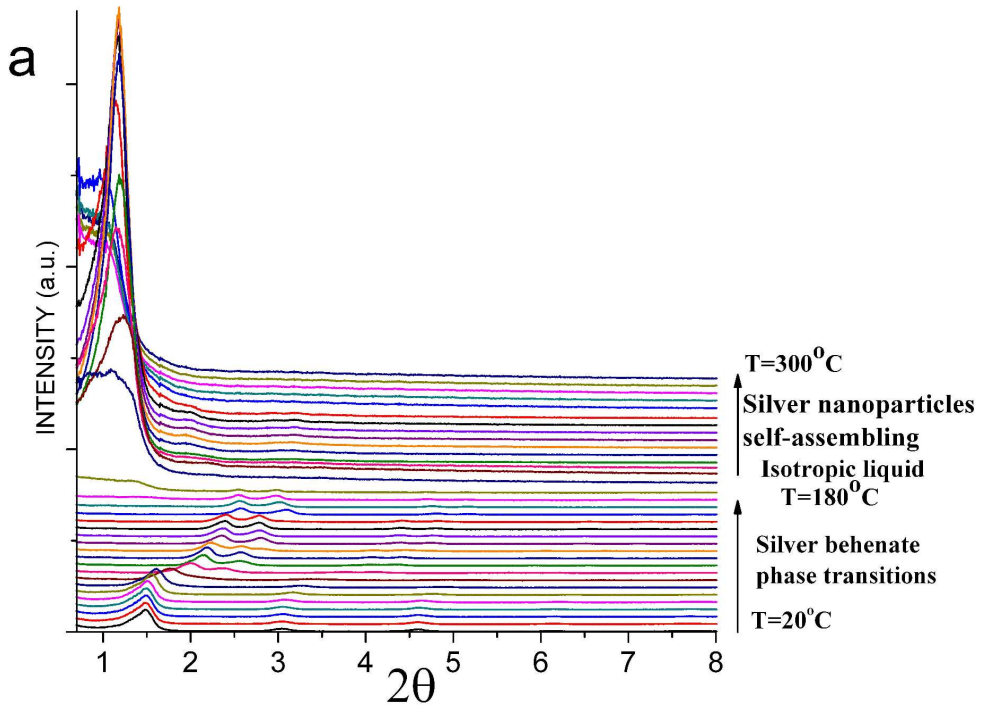
a
INTENSITY (a.u.)
T=300°C
Silver nanoparticles
self-assembling
Isotropic liquid
T=180°C
Silver behenate
phase transitions
T=20°C
1
2
3
4
5
6
7
8
2θ

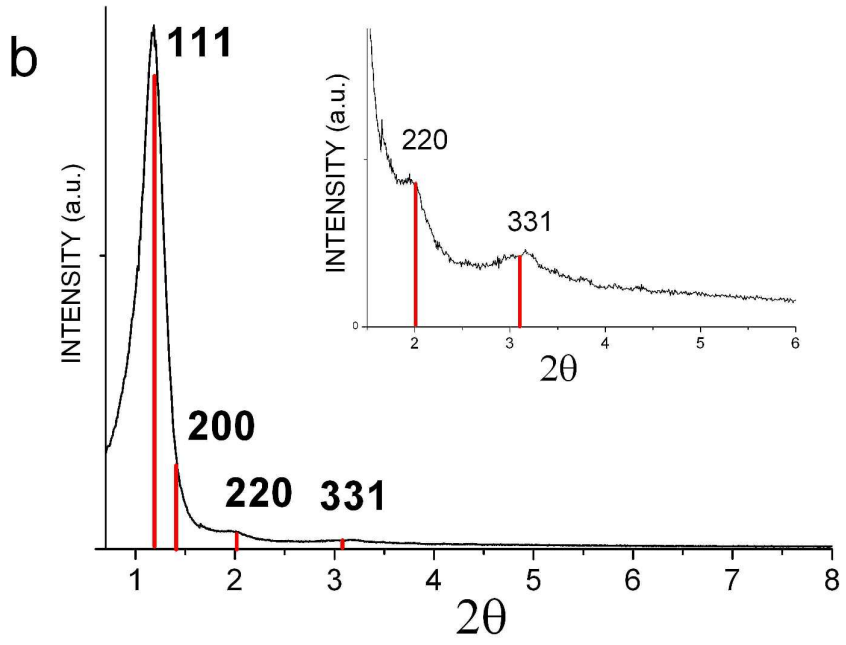
b
111
200
220
331
INTENSITY (a.u.)
1
2
3
4
5
6
7
8
2θ
INTENSITY (a.u.)
220
331
0
2
3
4
5
6
2θ

Figure S4.

a. *In situ* time-resolved X-ray diffraction patterns during thermal decomposition of silver behenate (C22). The changes in the diffraction patterns during heating from 20°C to 180°C are caused by multiple phase transitions of silver carboxylates into various liquid-crystalline states. The transition at ~180 °C is the conversion into an isotopic liquid, which is accompanied by the complete disappearance of Bragg reflections. The change of diffraction patterns during heating higher than 200 °C corresponds to the formation of ordered silver nanoparticles in an FCC nanostructure.

b. Small-angle X-ray diffraction patterns of self-assembled structures of silver nanoparticles forming during thermal decomposition of silver behenate (C22) at 250°C are indexed as an FCC structure. Magnified portions of diffraction patterns are shown in the inserts. Calculated unit cell parameter: a = 12.5 nm.

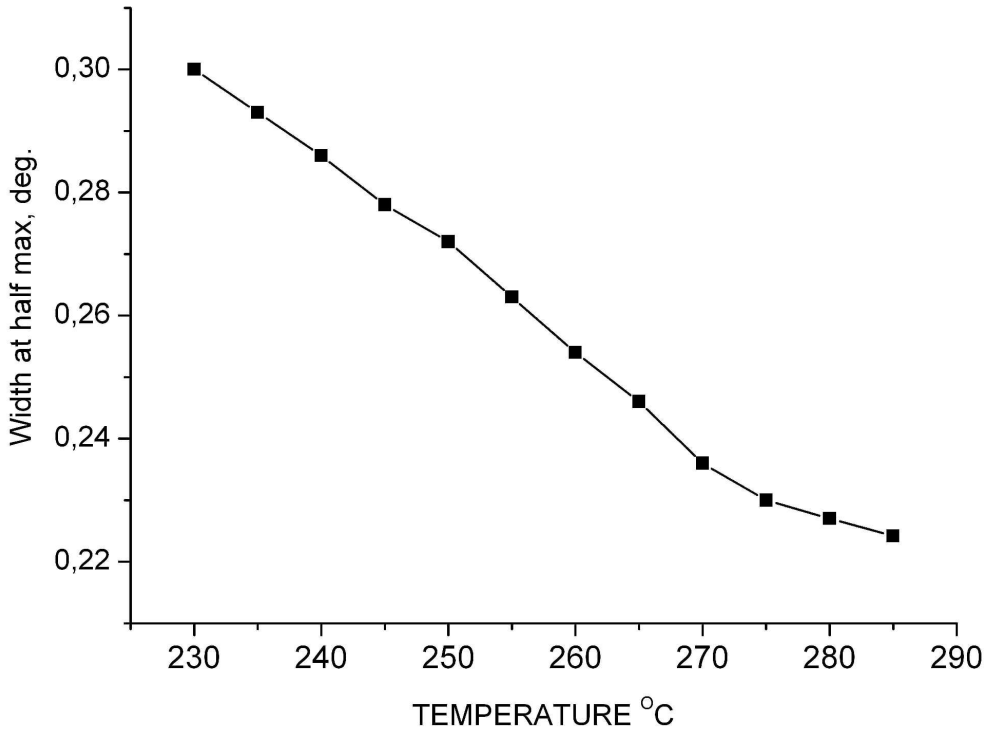

Figure S5. Evolution of FWHM of the (111) reflection of the supracrystal formed during thermal decomposition of silver stearate.

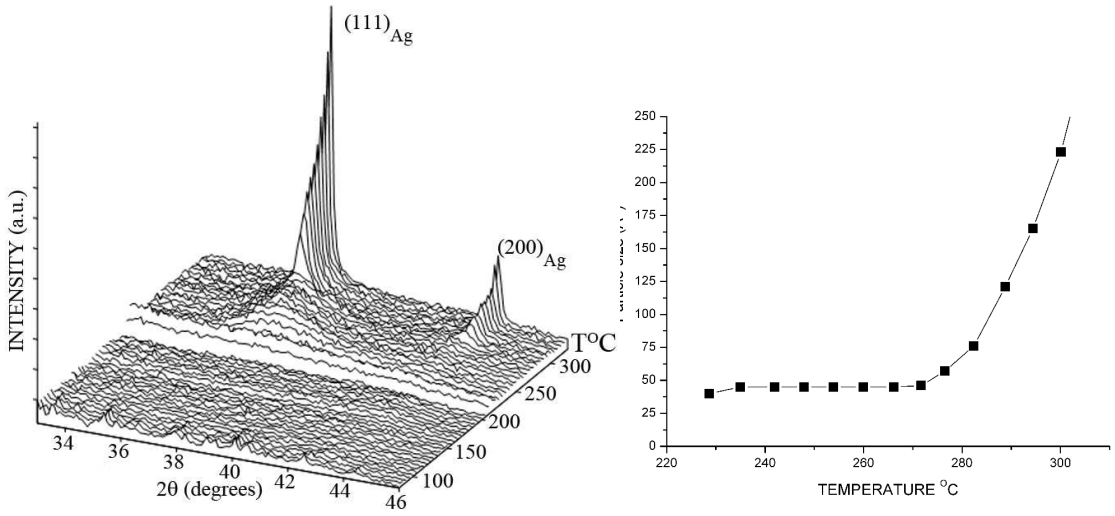

Figure S6. Evolution of the diffraction pattern in the 2θ=35-46 ° range during thermal decomposition of silver stearate and the calculated size of silver crystallites (Scherrer equation).

Supplementary Discussion

Formation, adsorption, and evaporation of carboxylic acid in the process of thermal decomposition of silver carboxylates

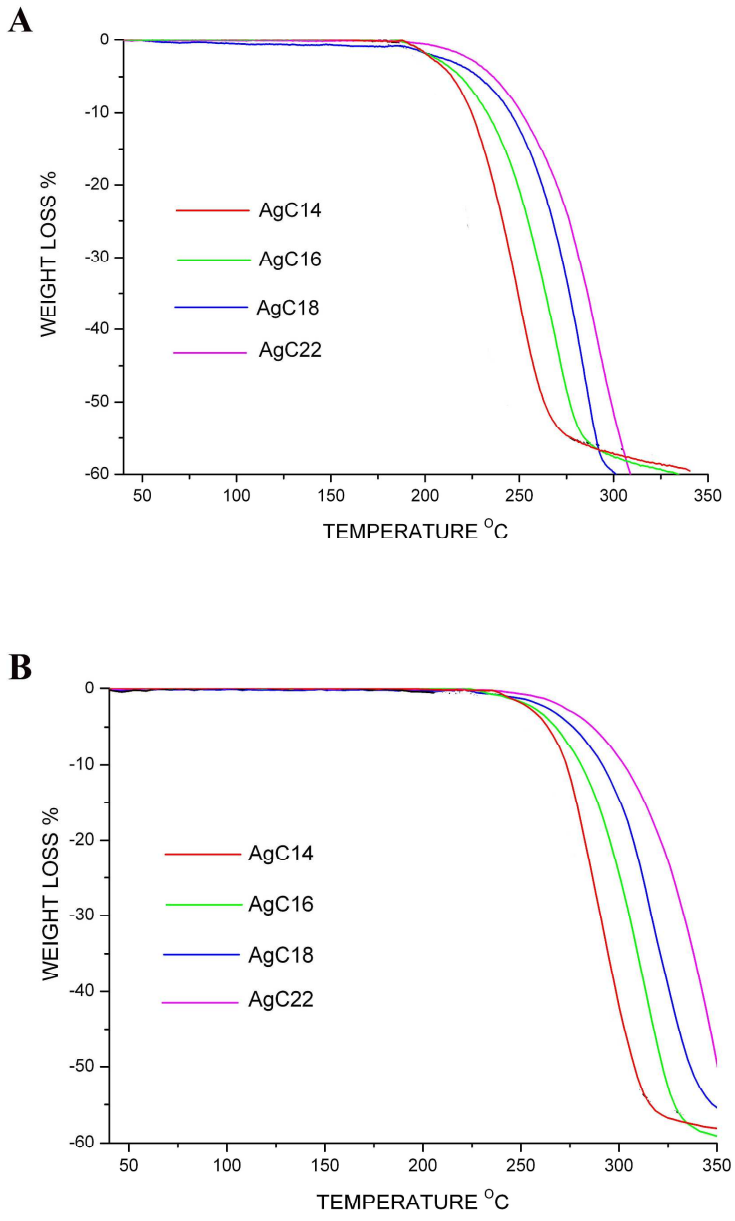

Figure S7. Thermogravimetric analysis of silver carboxylates at a heating rate of 10 C/min (A) and 20 C/min (B) under nitrogen.

Table S1

Weight losses of the silver carboxylate crystals heated up to 250^{o}C at different heating rates.

Silver carboxylate	Weight losses, %	
	10 deg/min	20 deg/min
AgC14	34	2.3
AgC16	20	2
AgC22	9	0.75

The formation of stearic acid in the process of thermal decomposition of silver stearate is confirmed by the following experimental data:

1. Direct evidence of stearic acid during thermal decomposition of silver carboxylates at 200°C is shown by the IR spectrum, which essentially overlaps the spectrum of the pure stearic acid. (Fig. S8).
2. DTA curves (Fig. S9) of the thermally decomposed silver stearate at 200^{o}C show an endothermic peak maximum at 69°C –70°C, which coincides with the melting temperature of stearic acid[1].

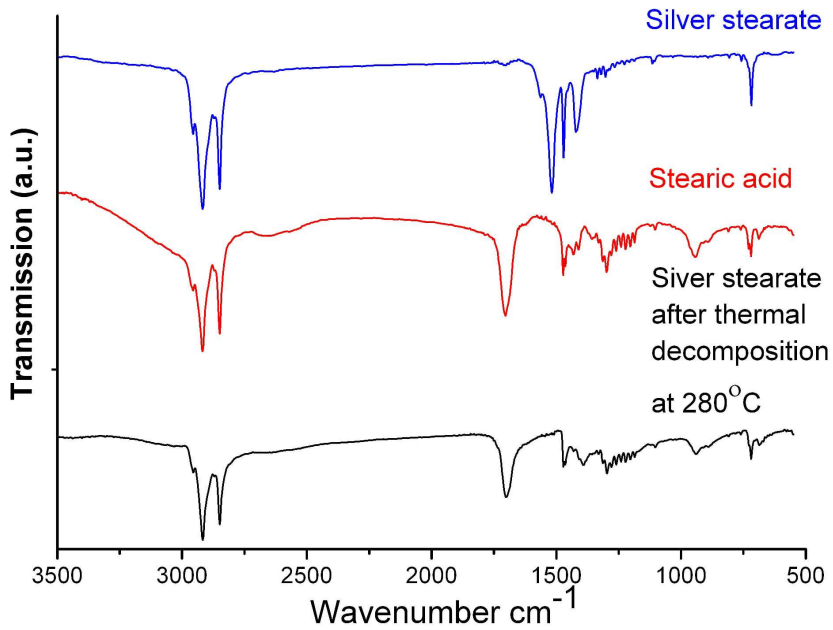

Figure S8. IR spectra of silver stearate (blue curve), pure stearic acid (red curve) and the by-product of the thermal decomposition of silver stearate (black curve) at 280°C.

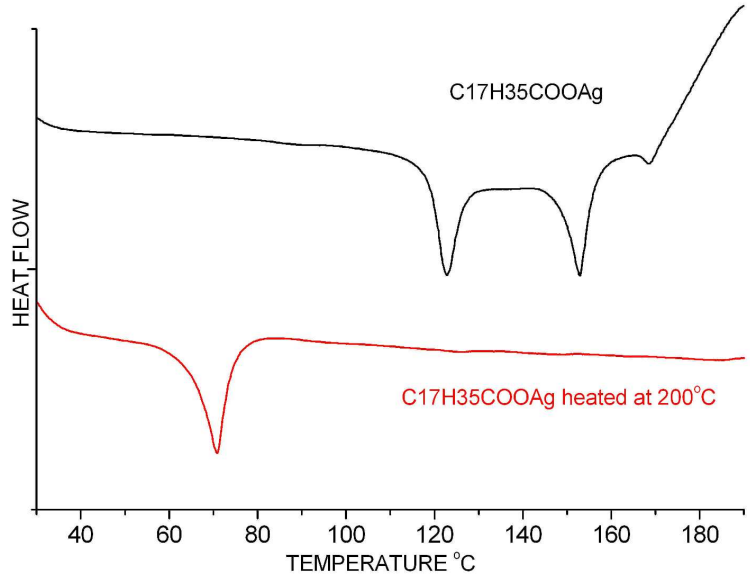

Figure S9. DTA curves of the initial silver stearate (black curve) and decomposed at 200 °C (red curve). The endothermic peak in the 70 °C is due to the stearic acid melting.

The evaporation of carboxylic acid in the thermal decomposition process (while the silver nanoparticles self-assemble) is confirmed by the weight change of the silver stearate during heating from 20°C to 300°C. Loss of carbon dioxide (according to the thermal decomposition equation: $2C_{17}H_{35}COOAg \rightarrow 2Ag + CO_2 + C_{17}H_{35}COOH + C_{17}H_{34}$) should show a 5.59% sample weight loss, although that weight loss would be 36.81% if carbon dioxide and unsaturated paraffin are both lost from evaporation. However, as seen from the TGA (Fig. S6), more than 50% is lost in the 200ºC to 350ºC range.

Similar results regarding the formation of behenic acid in the process of thermal decomposition of silver behenate were reported by Liu *et al.*[2]. It should be added that during the thermal decomposition of silver behenate, the most significant weight change also takes place during heating from 200°C to 300°C.

The possibility of saturated carboxylic (lauric and myristic) acids adsorbing on the surface of silver nanoparticles has been noted previously[3]. Additionally, it has been shown, that the decanoate-protected silver nanoparticles of 7.52 ±0.57 nm form orderly 2D nanostructures in the process of drying of colloidal solutions on carbon substrates[4]. Also, adsorption of the silver nanoparticles on Langmuir-Blodgett surfaces has been reported[5].

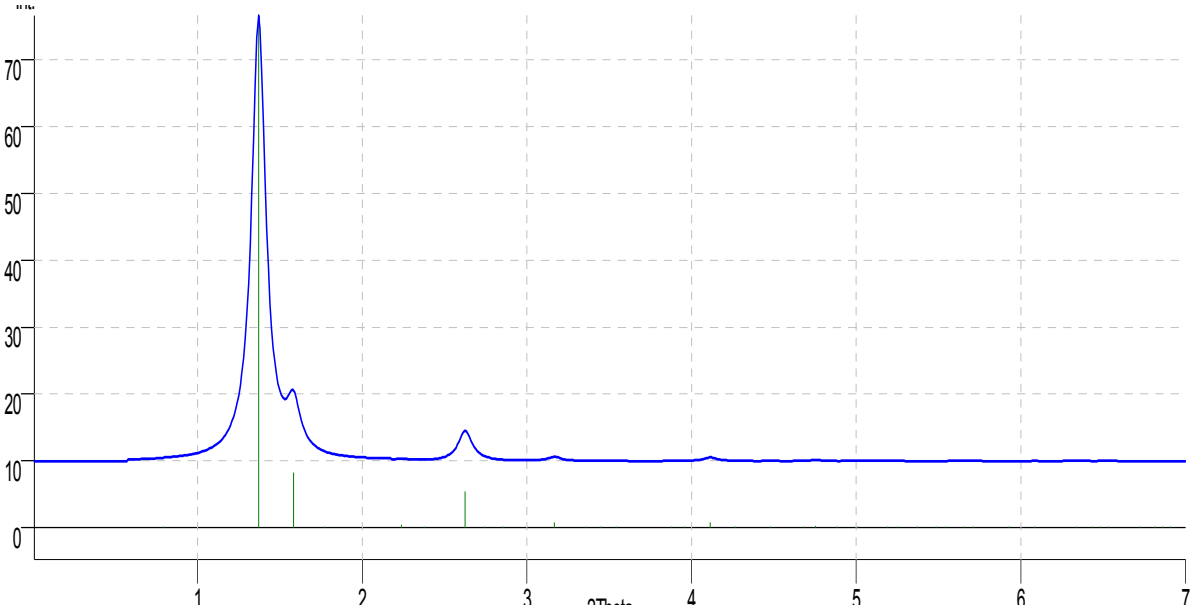

Figure S10. Calculated [6] X-ray diffraction pattern of the supracrystals (figure 6).

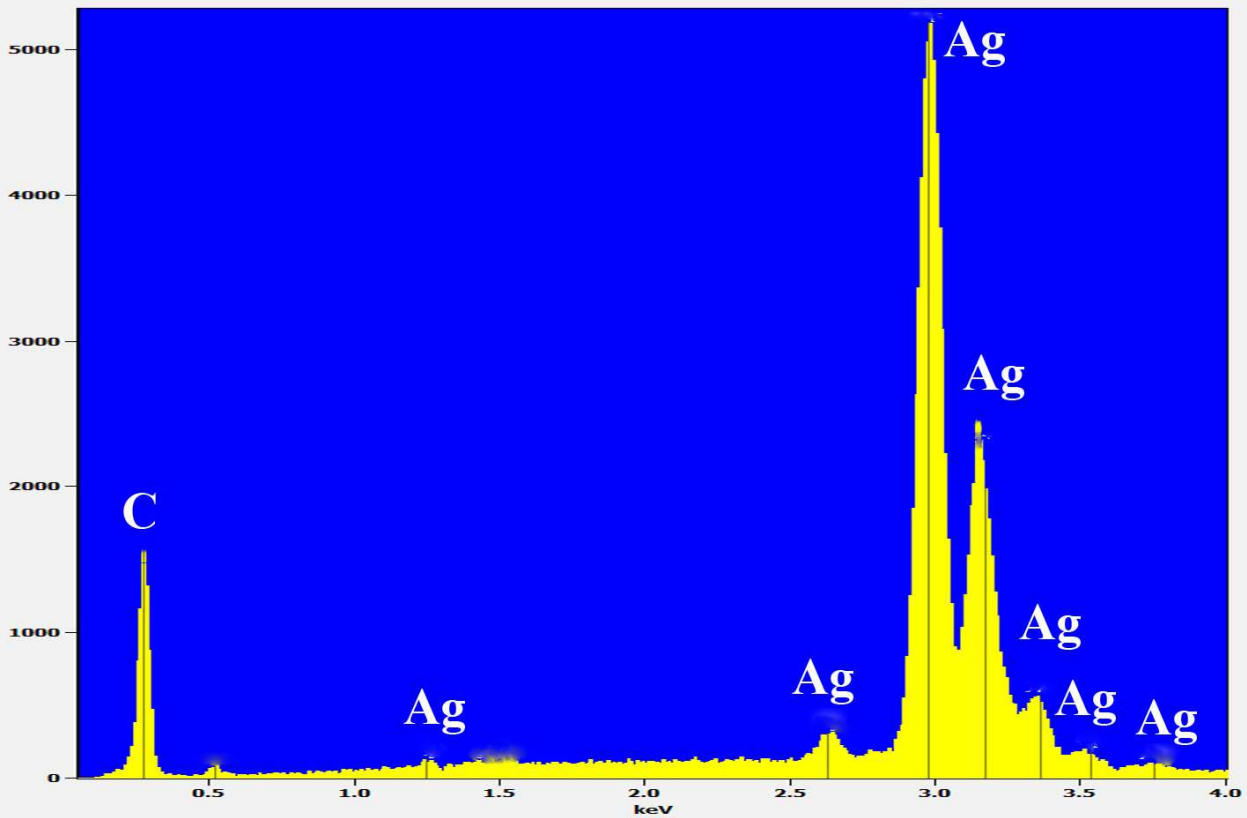

Figure S11. Energy-dispersive X-ray spectrum of the supracrystals.

Table S2.

Silver and carbon contents in the supracrystal.

Correction Method: Proza (Phi-Rho-Z)
Acc.Voltage: 30.0 kV Take Off Angle: 35.0 deg

Element Line	Wt.%	Error, %
C_K	28.44	1.35
Ag_L	71.56	1.95

References

1. Knothe, G., Dunn, R. O. A comprehensive evaluation of the melting points of fatty acids and esters determined by differential scanning calorimetry. *J. Am. Oil Chem. Soc.* **2009**, 86, 843–856.
2. Liu, X., Lu, S., Zhang, J., Cao, W. Thermal decomposition process of silver behenate. *Thermochim. Acta* **2006,** 440**,** 1–6.
3. Khanna, P. K., Kulkarni, D., Beri, R. K. Synthesis and characterization of myristic acid capped silver nanoparticles. *J. Nanopart. Res.* **2008,** 10, 1059–1062.
4. Dong, T-Y. *et al.* One-step synthesis of uniform silver nanoparticles capped by saturated decanoate: Direct spray printing ink to form metallic silver films. *Phys. Chem. Chem. Phys.* **2009,** 11, 6269–6275.
5. Sarkar, J., Pal, P., Talapatra, G. B. Self-assembly of silver nanoparticles on stearic acid Langmuir-Blodgett film: Evidence of fractal growth. *Chem. Phys. Lett.* **2005,** 401, 400–404.
6. Diamond. - Crystal and Molecular Structure Visualization. Crystal Impact - Dr. H. Putz & Dr. K. Brandenburg GbR , Kreuzherrenstr. 102, 53227 Bonn, Germany.